RSC Advances

ROYAL SOCIETY OF CHEMISTRY

www.rsc.org/advances

Controlled modification of starch in the synthesis of gold nanoparticle with tunable optical properties and its application in heavy metal sensing

Deependra Kumar Ban[1], Swadesh Kumar Pratihar[2], Subhankar Paul[1]*,

[1]Department of Biotechnology and Medical Engineering, National Institute of Technology Rourkela, Odisha, India.

[2]Department of Ceramic Engineering, National Institute of Technology Rourkela, Odisha, India

*Correspondence: Dr. Subhankar Paul, Associate Professor, Structural Biology and Nanomedicine Laboratory, Department of Biotechnology and Medical Engineering, National Institute of Technology Rourkela, Rourkela-769008, Odisha, India. E-mail: spaul@nitrkl.ac.in.Tel: +91-0661-2462284, +91-0661-2463284 (R).Fax: +91-0661-2462022.

Abstract

From environment perspective, green/semi-green synthesis method of nanoparticles is in great demand because of its non-toxic, eco-friendly nature and cheap synthesis method. In this study, we report the synthesis of gold nanoparticle (AuNP) of less than 20 nm average size by controlled modification of starch, which was used here as a reducing as well as the capping agent. The effect of various precursor concentrations and the role of reaction temperature on size, stability, and optical properties of synthesized gold nanoparticles (AuNP) were investigated. Various standard techniques along with surface plasmon resonance were analyzed for the characterization of AuNP. We observed that starch alone could induce the synthesis of AuNP in the presence of sodium hydroxide (NaOH) above 50^0C temperature. Varying starch concentration, reaction temperature, NaOH concentration were found responsible for tuning the size, fluorescence emission, and surface plasmon resonance. Thermo-gravimetric and FTIR analysis along with Benedict assay confirmed the modification in the starch structure during the AuNP synthesis. As an application, we demonstrated that our synthesized AuNP could sense the heavy metals Cu^{2+} and Pb^{2+} in ppm level through visible colorimetric change as well as SPR shifting. Therefore, our modified starch based semi-green synthesis method using starch as a reducing as well as capping agent and NaOH as a catalyst demostrated an environmental-friendly method of AuNP synthesis. Moreover, its application in heavy metal sensing can be used in industry for the detection of heavy metal presence in the contaminated water.

Keywords: Gold nanoparticle, Starch, Surface plasmon resonance, Fluorescence, X-ray diffraction, Heavy metal sensing.

Introduction

Due to excellent surface plasmon resonance and photoluminescence properties, gold nanoparticle has become a material of choice in various applications such as nanosensors [1, 2], electronic devices [3, 4], nanomedicine [5, 6], drug delivery [7, 8], and photothermal therapy [9]. To synthesize such nanoparticles for different applications, a number of methods like chemical, physical, and green route can be used to chemically reduce the precursor molecules. Among them, the green synthesis method has evolved as a method of choice due to the use of biocompatible molecules

to produce desired size, shape and functionalized nanoparticles with harmless byproducts. Although various groups have already used purified biomolecules like proteins [10], peptides [11, 12], carbohydrates [13], polyols [14], and polyamine [15] for the synthesis of gold nanoparticle (AuNP), the application of most abundant biomolecule in nature, i.e., carbohydrates have attracted special attention for its use in capping of various nanoparticles due to cost effectiveness and bio-friendly nature.

Furthermore, many groups already reported the synthesis of carbohydrate-based metal nanoparticles (silver, gold, platinum) by reducing respective metal salts in solutions using D-glucose as a reducing agent and starch as a capping agent, in these cases reaction was performed both at room temperature as well as elevated temperature [16-19]. In all these studies, starch has been used as a surface capping agent. However, its role as a reducing agent has yet not been evaluated. The reason may be the inertness of starch due to its linear chain amylose and a branched chain amylopectin component that causes steric hindrance due to intra-molecular interaction. However, it is possible that such inert starch can be activated by various physicochemical and mechanical methods to produce nanoparticle. Few studies have reported that modified form of starch was used as reducing as well as a capping agent for the production of various metal nanoparticles. These methods either used high pressure [20], various concentrations of alkali (0.01- 2M) with or without heating to modify starch [21, 22] and produced metal nanoparticles such as silver and gold. Furthermore, such starch-based synthesis method has so far not been reported of nanoparticles with size less than 20 nm. Moreover, such attempt results in the synthesis of polydispersed nanoparticles. Another problem-may be associated with the presence of excess starch in AuNP solution, which might interfere with the process during the use of nanoparticles in various applications. Moreover, in a recent report, excess starch was demonstrated to be separated by filtration [17]. However, filtration is likely to cause the possibility of removal of starch capped NP along with free starch.

Moreover, biocompatible nature of AuNP creates wide biomedical applications, which usually requires a non-toxic method to synthesis. Since, green synthesis approach always provides an additional advantage include avoiding toxic byproducts and hence, without further purification, such AuNP solution can directly be used for various biomedical applications. Therefore, it is

crucial to evaluate the role of starch as a reducing as well as a stabilizing agent in the synthesis of AuNP in an aqueous medium.

In the present study, we synthesized AuNP using gold salt ($HAuCl_4 \cdot 3H_2O$) as precursor molecules and starch as a reducing as well as capping agent (0.05-3%). We also evaluated the potential of NaOH (5-8 mM) as a reaction accelerator and starch modifier. The synthesized AuNP samples were further characterized using various standard techniques such as surface plasmon resonance (SPR), X-ray diffraction (XRD), dynamic light scattering (DLS), zeta potential (ζ), photoluminescence (PL), and thermogravimetric analysis (TGA). We further analyzed the potential of corn starch as a reducing as well as a capping agent of AuNP for the comparison with our present study mediated by potato starch. Further, to demonstrate the environment application of our synthesized AuNP, we also applied our NPs for heavy metal (Cu^{2+}, Ni^{2+}, Zn^{2+}, Pb^{2+}, Hg^{2+}, and As^{5+}) sensing by detecting visible color change and SPR shift.

Experimental Section

Materials

$HAuCl_4 \cdot 3H_2O$ (auric chloride) was purchased from Sigma-Aldrich, NaOH and starch were purchased from Himedia, India and used without further purification. Heavy metals such as $CuSO_4$, Ni $(CH_3COO)_2 \cdot 4H_2O$, $ZnSO_4 \cdot 7H_2O$ were purchased from Merck pvt. Ltd and Pb $(CH_3COO)_2 \cdot 3H_2O$, $HgSO_4$, $Na_2HAsO_4 \cdot 7H_2O$ from Loba Chemie Pvt. Ltd, India. All the plasticware were purchased from Tarson, India and glassware were purchased from Borosil, India. Before use, glass wares were cleaned using aquaregia and Milli-Q water. Milli-Q water was used throughout the study. The solution was filtered using 0.2 μm membrane filter (Millipore, India).

Synthesis of gold nanoparticle

For the synthesis of AuNP, we prepared 1.0% (w/v) starch solution in Milli-Q water by heating in a microwave oven for 1 min. In the clear soluble starch solution, we added 1.0 mM auric chloride and heated at 70 ^{0}C for 5.0 min with constant stirring. After heating, NaOH (6.0 mM) solution was added to auric chloride solution within 2 min. The reaction proceeded for further 40 min and cooled down to room temperature (RT). The AuNP solution was kept in freeze at -20^{o}C for 1 h and thawed. This process precipitated the excess starch along with large size AuNP. The solution was centrifuged at 10,000 rpm for 10 min and supernatant was separated. This process was repeated three times to get a clear AuNP solution. The various parameters like temperature (RT, 40, 50, 60, 70, 80 ^{0}C), concentration of auric chloride (0.2, 0.5, and 1.0 mM), NaOH (2.0, 3.0, 4.0, 5.0, 6.0, 7.0, 8.0, 10, 20, 50, and 100 mM), and starch (0.05, 0.1, 0.2, 0.5 1.0, 2.0, and 3.0% w/v) were optimized. We also performed two more experiments; first with cornstarch with 6.0 mM NaOH and second with cornstarch with D-glucose and NaOH. The purpose was to explore the potential of the method with another type of starch such as corn starch (besides commonly used potato starch) and potential of NaOH in speed up the D-glucose based reduction process which was a slow process at the room temperature (RT).

Characterization of AuNP

UV-VIS spectroscopic analysis

The surface plasmon resonance (SPR) of AuNP was analyzed by UV-VIS spectrophotometer (Perkin Elmer, λ-35). The sample was prepared in Milli-Q water (18 mΩ) and scanned in the range of 200-700 nm, with a slit width of 2.0 nm and scanning speed of 100 nm/min. All the spectra were baseline corrected and plotted against wavelength.

Electron Microscopy Imaging

The samples were diluted and prepared on a silicon wafer by drop casting method and dried in a vacuum drier. The dried samples were gold coated for 30 seconds and analyzed. In addition, to perform the TEM analysis, AuNP sample was diluted with Milli-Q water and deposited on a copper grid (300 mesh) by drop casting method and dried in the vacuum. Transmission electron microscopic analysis of AuNP sample was performed by TEM (Jeol, JEM-2100F).

Fluorescence spectroscopic analysis

The fluorescence measurement of AuNP was performed by Cary eclipse spectrofluorimeter. The emission of the sample was recorded by exciting at 490, 500, 510, and 520 nm at a slit width of 10 nm for both excitation and emission. The emission spectra were recorded, and normalized emission spectra were plotted for analysis.

X-ray diffraction analysis

All the samples were deposited on the quartz slide and dried in vacuum. The baseline correction of spectra was done using a quartz slide. The samples were analyzed using XRD (XRD ULTIMA-IV, Rigaku, Japan) in the range of 25- 90^0, with 2θ/min scanning speed (2θ is scattering angle) and 0.5° step size. The peak position was matched using JCPDS card No. 4-0784 for gold. The crystallite size of AuNP samples were calculated using Scherrer's formula: $D = 0.94\lambda / \beta (1/2 \cos\theta)$; where λ is wavelength (1.54 A), β is line broadening, θ is Bragg's angle.

Dynamic light scattering

The hydrodynamic size of particles was measured with respect to the 'number percent of nanoparticles' by Zeta Sizer (Nano-ZS, Malvern pvt. Ltd.). Simultaneously, stability of nanoparticles was analyzed by zeta potential analysis. Transparent samples were prepared in Milli-Q water and analyzed. The data was analyzed using DTS 7.0 software provided by the company.

Thermal analysis of AuNP

The weight percent of starch on AuNP was analyzed by thermogravimetric analysis using Netzech DSC/TGA instrument in an oxygen environment. Starch and AuNP used were more than 1 mg, which was a minimum weight limit for analysis. The samples were heated in the range of 25 ^{0}C to 700 ^{0}C, at a rate of 10 ^{0}C/min. The air was introduced into the sample chamber during measurement, at a rate of 25 mL/min, which was sufficient to remove oxidation products without any buoyancy effect. The percentage mass change of starch and AuNP was normalized and analyzed the thermal profile of particle. The weight change of the samplewas calculated with regard to the initial mass.

FTIR analysis of modification in starch

The structural modification in starch due to heating (60-80^{0}C) and the presence of NaOH was monitored by FTIR spectroscopy (Alpha-series, Malvern). The analysis was performed in the range of 500-4000 cm^{-1} with 2 nm resolution and average of 25 scans was evaluated for various vibrational bond analyses. We compared the transmission mode of starch without modification and after the heat and NaOH treatment. The transmission data of all the samples were analyzed. The baseline correction was performed with respect to water.

Heavy metal sensing assay

The colorimetric and SPR based heavy metal sensing using synthesized AuNP was performed for copper (Cu^{2+}), nickel (Ni^{2+}), zinc (Zn^{2+}), lead (Pb^{2+}), mercury (Hg^{2+}), and arsenic (As^{5+}) detection in water using the compound $CuSO_4$, Ni $(CH_3COO)_2 \cdot 4H_2O$, $ZnSO_4 \cdot 7H_2O$, Pb $(CH_3COO)_2 \cdot 3H_2O$, $HgSO_4$, and $Na_2HAsO_4 \cdot 7H_2O$, respectively. The assay was performed using a different dilution of transparent 200 ppm stock solution of the heavy metal compound prepared in Milli-Q water. Initially, 50 ppm of metal compound was mixed with 100 μM of a AuNP solution and incubated for 10 min. Visible color change was monitored,and SPR was measured for all samples. Moreover, different cocnentration of heavy metals (1-50 ppm) were also used with fix cocnentration of AuNP (75μM).

Results and Discussion

To synthesize the AuNP of below 20 nm average sizes, we varied different parameters such as concentration of NaOH, starch, gold salt and reaction temperature. The excess starch was removed by keeping the solution at -20^{0}C for 1 h followed by thawing and centrifugation at 10,000 rpm for 10 min. The effect of various parameters on the synthesis of AuNP was discussed in the following sections.

Effect of NaOH concentration

The different concentration of NaOH (2.0, 3.0, 4.0, 5.0, 6.0, 7.0, and 8.0 mM) with 1% starch (w/v) was used in the synthesis of AuNP when 1.0 mM of auric chloride was used as initial precursor concentration at 70^0C (Fig.1). Here, we found that the use of increasing NaOH concentration like 2.0, 3.0, and 4.0 mM resulted in a gradual change in color from yellow to light black. However, when 5.0 mM NaOH was used, the solution color initially turned black. However, it turned dark ruby red after a while. Further increasing of NaOH concentration to 6.0, 7.0, and 8.0 mM revealed no further change of ruby red color, indicates that the use of NaOH above 5 mM showed the ability to produce AuNP while increasing concentration of NaOH demonstrated speed up the reaction rate. The SPR analysis also showed a red shift from 516 nm to 544 nm of an absorption peak indicates forming of larger size of the particle (Fig.1A). When, we plotted the SPR shift with respect to NaOH concentration and interpolated it within the working range of NaOH concentration (Fig. S1. A), we found a red shift in SPR for NaOH concentration of below 5.0 mM while the use of 5.0 and 6 mM of NaOH exhibited blue SPR shift.

Further increase of NaOH concentration i.e., 7 and 8 mM showed slight red shift (Fig. S1. A). The fact collectively proved that the synthesis of AuNP and reaction rate was dependent on NaOH concentration. However, below and above a range of critical value of NaOH concentration, the synthesis of AuNP either not significant (below 5.0 mM) or produced larger particles (above 8.0 mM) as shown by the variation in SPR shift and color change. It was found that the application of higher concentration of NaOH (i.e. above 8 mM) caused immediate color change and for 20 mM or above, color turned from violet to black (Supplementary Fig. S3A). This proves that the NaOH accelerates the synthesis of AuNP while higher concentration speeds up the reaction rate and produces larger AuNP.

The dynamic light scattering (DLS) analysis was also performed to analyze the hydrodynamic diameter of AuNP population. The intensity of mean number percent with respect to hydrodynamic size and peak width was analyzed (Fig. 1C). The results revealed that NaOH concentration was critical for the synthesis of a higher population of AuNP with less than 20 nm

and low polydispersity. When NaOH concentration was below a critical value (i.e. less than 5 mM), the larger particles were produced, however increasing NaOH concentration to 6 mM produced AuNP with smaller size (10-20 nm). To monitor the stability of the suspension, when zeta potential was measured, we found that the stability was highest at NaOH concentration of 5 and 6 mM (-25 to -20 mV). Further increase of NaOH concentration, i.e., 7 and 8 mM produced AuNP of larger size, higher polydispersity and reduced stability (Fig. S1C).

Therefore, the overall experimental results indicated that for obtaining reduced size with high stability, the critical concentration of NaOH was required.

Figure.1

Effect of reaction temperature on SPR

To understand the role of reaction temperature, we also performed the reaction at room temperature (RT i.e. 25^0C), 50^0C, 60^0C, 70^0C, and 80^0C (Fig.1. B and D), when other parameters were constant (1.0 mM auric chloride, 1% starch, and 6 mM NaOH). When we performed the reaction at RT and below 50^0C for more than 1.0 h, we found that the solution became transparent after addition of NaOH (6 mM), and no significant color change was observed. However, when the reaction was performed at 50^0C or above, the solution was initially found transparent, however, turned black thereafter, and finally turned ruby red after 40 min of reaction, indicated the synthesis of AuNP (Fig. 1. B).When, we plotted the temperature against SPR peak, we found that below 60^0C (i.e. RT and 50^0C) and above 70 ^{0}C (i.e. 80^0C), the SPR peak showed redshift (Fig. S1. B) while reaction below critical temperature (50^0C) revealed slow reaction rate.

However, when the reaction was perforemd at 80^0C with 5-8 mM of NaOH, 1% starch and 1 mM of gold salt, the reaction rate was fast. It reveals that the reaction requires minimum activation energy, however, the energy achieved was less by lower NaOH concentration (below 10 mM) and hence the reaction needed to be performed above 50^0C to overcome such threshold

energy barrier. However, temperature above 80^0C perhaps caused a rapid burst of the nucleus and uncontrolled growth of particles that consequently produced poly-dispersity. In fact, the above result was also supported by the analysis of hydrodynamic size distribution (Fig. 1 D) and zeta potential (Fig. S1D) measurement of AuNP suspension. It showed that at higher temperature (i.e. more than or at 80^0C) larger particle was formed with less stability while in the range of 60-70 ^{0}C more population of smaller particle of 10-20 nm mean size were formed with higher stability (Fig. 1D & Fig. S1D).

The effect of starch concentration

Further, we wanted to know the role of starch in controlling AuNP size when other parameters were kept constant (1.0 mM auric chloride, 6 mM NaOH, and reaction temperature at 70^0C). Fig. 2A and C, showed how the variation in starch concentration affects SPR and subsequently the size of NP, which was further confirmed by color variation and DLS data. The SPR analysis also revealed that at a lowerconcentration, larger particles was synthesized (shown by violet color for 0.05 % starch concentration) (Fig. S3. B). With the increase of starch concentration,i.e., from 0.1 to 3%, AuNP solution turned light to dark ruby red indicates a synthesis of small particles. When SPR was analyzed between starch concentrations of 0.05 to 3%, it showed initially a blue shift in SPR up to 0.2 % with an increase of SPR up to 1% of starch (Fig. 2. A), However,become constant thereafter till 3% (Fig. S2. A) starch.A comparitive study was performed using corn starch (0.2%) with the existing potato starch with and without D-glucose. It showed that corn starch-based synthesized AuNP without D-glucose showed relatively narrow SPR peak (Fig. S3. C) than the synthesis method using D-glucose (Fig. S3. D).This fact further validated that potato starch (reduction and capping) with NaOH for AuNP synthesis not only compatible with other starch but also eliminate the use of D-glucose in reduction process and other buffer ingredients to produce smaller size of AuNP.

Further, we also analyzed the hydrodynamic size distribution with different starch concentration (0.2-1%). The results showed that increasing starch concentration from 0.2-1% also decreased the size of AuNP and produced a higher percentage of small particles (Fig. 2. C). We also found that increasing starch concentration also increased the zeta potential of AuNP and stabilized the suspension up to 1% of starch (Fig. S2. C). The initial shift of SPR was found up to 0.2% (shown

by violet color for 0.05% and ruby red for 0.2%) of starch but a further increase of starch produced a larger population of small particles. However, DLS analysis showed that slight red shift in SPR also indicated the presence of a higher concentration of surface capping species on the particles that caused a slight red shift. Moreover, the use of 1% to 3% starch demonstrated no significant shift in SPR, which indicated the saturation of AuNP for further interaction with available starch concentration. A further role of starch concentration was also observed during retrogradation of starch (Fig. S6). We found that lower concentration of starch was unable to stabilize the AuNP during freezing and thawing and produced particle suspension with violet color due to aggregation. Higher concentration, i.e., above 1% of starch, however, caused a higher amount of AuNP precipitation with starch although color variation was not found.

Figure 2

The effect of gold chloride

The effect of various concentration of gold salts was also analyzed when other parameters were constant (1% starch, 6mM NaOH, and reaction temperature at 70^0C). The results showed that SPR of various AuNP solutions varied with gold salt concentration exponentially (data below 0.5 mM and above 1 mM of AuNP was not shown). However, no significant change was found up to 0.5 mM of gold salt (Fig. S2B). The DLS analysis showed that both 0.5 mM and 1 mM concentration of gold salt produced AuNP of equivalent hydrodynamic size of 10-15 nm (Fig. 2D) with a slighly broad peak width for AuNP synthesized from 0.5 mM gold salt.The zeta potential analysis also showed no significant change in stability of AuNP, as both the sample showed zeta potential approximately of -20 eV(Fig. S2D).

Electron Microscopic Analysis

FESEM analysis of AuNP under various conditions and TEM imaging of the AuNP sample with the optimum condition (1 mM $HAuCl_4.3H_2O$, 6mM NaOH, 1% starch) was performed (Fig. 3A-F). The results showed that AuNP synthesized from 0.5 mM of auric chloride contains smaller particles (Fig. 5A). However, AuNP synthesized using 1.0 mM gold salt produced larger

particles with less polydispersity (Fig. 3B). In both cases, 6.0 mM NaOH and 70 ^{0}C reaction temperatures were used. However, when NaOH concentration was increased to 8.0 mM, the AuNP image revealed the formation of a large particle with high polydispersity and irregulars shape (Fig. 3C). When AuNP was prepared at high-temperature like 80^{0}C, the process produced larger particles with spherical shape (Fig. 3D) and little polydispersity. Furthermore, starch precipitate with AuNP was also analyzed (Fig. 3E), which showed large and randomly distributed starch granule. The TEM analysis of optimized sample was performed (Fig. 3F), which revealed small AuNP of 7-10 nm size.

Figure 3

X-Ray diffraction analysis:

XRD analysis was performed to observe the characteristic crystallite size and the effect of various parameters on the growth of AuNP crystallite size (Fig. 4). The peak broadening and peak shift of AuNP signified the decrease in the particle size. The data were analyzed by background subtraction and fitting of peaks. From Fig. 4, we observed that the lattice points were located at 111, 200, 220, 311 positions with some peak shift and peak broadening. These lattices were points matched with JCPDS card No 4-0784, which confirmed the face centered cubic structure of the sample. The peak broadening at various positions indicated the formation of AuNP. The sample with different concentration of NaOH (5, 6, and 8 mM) showed peak broadening which varies with the concentration of NaOH (Fig. 4 A, C, and H) and showed crystallite size of 13.76, 7.95, and 14.56 nm, respectively. Moreover, we also analyzed the effect of various temperatures (60, 70, and 80 ^{0}C) on the AuNP crystallite size (Fig.4 C, D, and E) that showed crystallite size of 8.68, 7.95, and 18.62 nm, respectively. We found that AuNP produced at higher temperature demonstrated narrow peaks, which signified the synthesis of larger particles.

Furthermore, we also analyzed the effect of various concentration of starch (0.5, 1 and 2%) (Fig. 4C, F, and G) which showed AuNP crystallite size of 6.84, 7.95, 7.55 nm, respectively and gold salt (0.5, and 1 mM) (Fig. 4B and C) that showed AuNP crystallite size of 7.16, and 7.95, respectively. We observed that increasing concentration of starch to 2% reduced the intensity of peak at 200, while variation in gold salt concentration showed little shift in peak at 200 and reduced intensity of peak at 220, and 311. The crystallite size of AuNP samples were analyzed using Scherrer's formula: $D = 0.94\lambda / \beta (1/2 \cos\theta)$; where λ is wavelength of X-ray (1.54 A), β is line broadening, θ is Bragg's angle. The peak measured at 38°, 44°, 64°, and 77° were used for crystalilite size analysis using Scherrer's formula, and an average of crystallite size (nm) obtained by analysis of all four peaks was represented as crystallite size of AuNP in nm.

Figure 4

FTIR and Thermogravimetric (TGA) analysis

To analyze the structural change in starch on the AuNP surface, we performed FTIR spectroscopy and TGA analysis. The structural changes and variation in bending of bonds due to heating and NaOH treatment were analyzed by FTIR spectroscopy in ATR mode. We found that short period of treatment of starch in microwave irradiation and further heating at 50^0C or above with different concentration of NaOH caused a structural modification in starch. FTIR analysis of native starch demonstrated no sharp peak, however, peaks between 907-1106 cm^{-1} showed crystalline nature of starch with water content[25] and reduction in peak intensity indicate reduction in crystallinity (Fig. 5A). The peak between 1133-1158 cm^{-1} was due to C-OH bond, 1347-1420 cm^{-1} for COO^- group, 1425-1580 cm^{-1} for CH_2 in aliphatic and 1582-1700 cm^{-1} was the peak of water and free OH group. The peak between 2743-3000 cm^{-1} represented CHO and CH_3-a group with bending, 3515-3600 cm^{-1} of OH in alcohol[26]. Starch with NaOH and heating resulted in reduced peak between 907-1106 cm^{-1} that indicated reduced crystalline nature of starch (Fig. 5A). The peak between 2500-3100 cm^{-1} was found narrow, and other peaks between 3200-3800 cm^{-1} either were less intense or missing (Fig. 5A). Here, we conclude that treatment of starch with mild alkali and heating perhaps modified the structure of starch molecules, which

were perhaps responsible for the active nature of starch in nanoparticles. Further, we also analyzed the effect of various conditions for starch solubility and analyzed by FTIR spectroscopy (see Fig. S4).

Furthermore, we wanted to analyze the cause of variation in FTIR spectra of modified starch. Such change could be due to the change in the conformation of amylose and amylopectin or due to the production of new reducing species [21, 22]. Semi-quantitative Benedict assay was performed with starch solution treated with 7 mM of NaOH and heated at 70^0C (Fig. S5) and compared the color variation with a known concentration of D-glucose. The result showed that treatment of starch with 7 mM of NaOH and heating produced approximately 0.2% of reducing species (shown by green color of Benedict solution with starch), while only heat-treated starch solution and the starch solution treated with 3 and 4 mM NaOH was unable to produce sufficient amount of reducing sugar (Fig. S5).

Accordingly, we proposed a mechanism of AuNP synthesis involving heat-mediated modification of starch in the presence of NaOH. Initially, when starch was heated, it caused the starch structure to open (amylose and amylopectin) while the addition of NaOH by alkalization of hydroxyl group activated the starch molecule and produced reducing species. When gold salt was added to the activated starch solution, excess NaOH first reacted with gold salt to produce hydroxyl intermediate $Au(OH)_x$ which further reacted with the reducing species of the starch molecule and produced AuNP nucleus. AuNP nucleus was grown further to produce AuNP. When, excess NaOH was added with heating, it produced a higher order of $Au(OH)_x$ that caused rapid growth and production of large particles[22]. At low temperature, the generation rate of the nucleus was slow and required a larger amount of NaOH for starch modification while heating with various concentration of NaOH (5-8 mM) rapidly produced the reducing species. Moreover, unreduced starch acted as a capping agent and prevented the production of larger particles due to heating. However, heating with a higher concentration of NaOH reduced to a high extent and hence less amount of unreduced starch was present for capping. Ji et al and Zhang et al reported that reaction of NaOH with auric chloride produced intermediate gold hydroxide that caused conversion of yellow color to transparent and the order of gold hydroxide increased from 1.0 to 4.0 with increasing the NaOH concentration. Moreover, higher order of Au(OH)x was responsible for the different redox potential and reduction rate of gold [23,24]. The plausible

reaction mechanism of AuNP synthesis was represented below while detail of reaction with hydroxyl intermediate formation and higher order of gold chloride hydroxide was given in supplementary information (supplementary data Section.4):

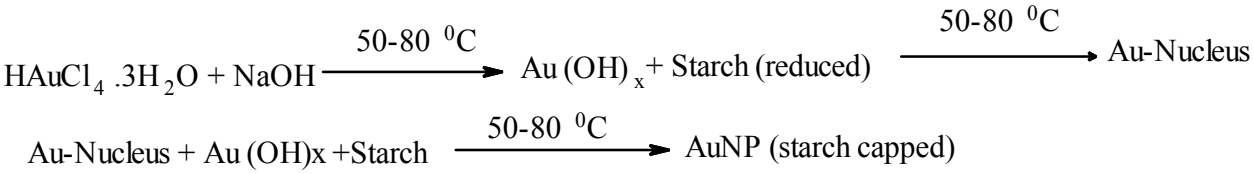

Figure 5

Moreover, to analyze the amount of starch on the synthesized AuNP, the thermal analysis of starch capped AuNP was perforemd in the range of 25 to 700°C with 10°C/ min step size in an oxygen environment. The results confirmed the unbound and bound water loss and showed starch degradation up to 250°C (Fig. 5B). The analysis demonstrated that the starch degradation above 250^{0}C took place in two steps; a fast phase from 250 to 350°C followed by a sluggish phase from 350 to 500°C. We also analyzed thermal degradation behavior of AuNPs under the same condition, i.e., above 250°C. It showed one phase of mass loss up to 200°C and again a sharp fall at 600°C, beyond which no mass change was observed. The fact indicated the absorption of starch on the surface of AuNP. However, the absence of a second phase in the AuNP sample showed only one type of the starch component was attached. From TGA analysis, we can conclude that modification of starch produce both stable and unstable form of component in solution. Moreover, retrogradation process may enhance the tendency of the unstable component to be precipitate out that resulted in stable form of starch remain in solution and act as capping agent.

Fluorescence spectroscopy analysis

Further, we wanted to analyze fluorescence emission, another important optical property of AuNP, which is sensitive to size, shape, capping agent, and the environment change around AuNP. We measured the fluorescence spectra of various AuNP samples by exciting samples at 500 nm (Fig. 6 A-C). AuNP prepared using 1 mM gold salt and 6 mM NaOH at 70°C with 1% starch also excited at 490, 500, 510 and 520 nm (Fig. 6D). Fluorescence emission of AuNP showed slightly red shift at excitation wavelength of 500 nm for sample with different NaOH concentration (Fig. 6A) while increasing starch concentration (Fig. 6B) and temperature (Fig. 6C) showed large red shift. However, the excitation at 490, 510, and 520 nm demonstrated no significant shift for these samples. When AuNP (1 mM $HAuCl_4.3H_2O$, 1.0 % starch, 6.0 mM NaOH, and 70^0C) was excited at 490, 500, 510, and 520 nm, it showed shift in emission spectra for each excitation wavelength. It was also a well-known fact that fluorescence of AuNP depends on the size, shape, surface functional group (type and density) and polarity of the solution environment. Hence, our results revealed that fluorescence property of AuNP can be tuned for each excitation of AuNP by co-stabilizing using NaOH and starch.

Figure 6

Heavy metal sensing

We also wanted to evaluate the application of our synthesized AuNP (size 7-10 nm, Fig. 3F) in the sensing of six heavy metals using optical properties (colorimetric and SPR). Colorimetric sensing and SPR analysis with 50 ppm of Cu^{2+}, Ni^{2+}, Zn^{2+}, Pb^{2+}, Hg^{2+}, and As^{2+} revealed that starch capped AuNP (100 µM) was most sensitive with Pb^{2+} and Cu^{2+} (Fig. 7A and B) and less or insensitive to other four metals (Fig. S7). When different concentration of Pb^{2+} (1-20 ppm) and Cu^{2+} (10-50 ppm) were mixed with 75 µM of AuNP solution and incubated for 10 min, the change in color from pink to dark ruby red for Pb^{2+} and violet color for Cu^{2+} was observed. The SPR shift and peak broadening was also observed, which signified the formation of larger particles (Fig. 7A and B). Simultaneous analysis of other metals revealed no significant color change of AuNP solution but showed a red shift in SPR with peak broadening except Hg^{2+},

which showed blue shift (Fig. S5). Therefore, although, in this study, we found that our AuNP demonstrated sensitivity to both heavy metal ions Cu^{2+} and Pb^{2+}, sensing to Cu^{2+} was strongly monitored by visible color change.

Figure 7

Multiple reports have been documented about the mechanistic proposal, which explained that affinity-based chelating activity of surface capping agents was responsible for sensing the metal ions [27-29]. Such chelating effect subsequently triggers aggregation among capped nanoparticles that produced a change in colorimetric and SPR signal. In our study, the capping agent starch might be responsible for such preferential chelating of metal ions [30] such as Cu^{2+} and Pb^{2+} (Fig. 8). However, the specific type of metal ions to be chelated perhaps is dependent on the kind of capping agents used that produces various level of affinity towards heavy metal ions as well as the size and shape of AuNP. A representative scheme for themechanism of action was shown in Fig. 8.

Figure 8

Conclusion

In this work, we reported the synthesis and characterization of stable AuNP of controlled size by modulating various parameters such as concentration of auric chloride, starch, NaOH and reaction temperature. We demonstrated that starch alone could reduce $HAuCl_4.3H_2O$ in the presence of NaOH and at a reaction temperature of 50^0C and above. The FTIR analysis and Benedict assay confirmed a modification in starch structure and production of reducing agents. Hence, we confirmed that starch here acts as a reducing as well as capping agent. Moreover, we found that NaOH and starch provided stability to AuNP in the concentration range of 5.0-7.0 mM and 0.2-1%, respectively. This work also demonstrated that NaOH could accelerate the reaction rate by catalyzing the reaction and play a crucial role in the production of reduced form

of the starch molecule that further helps in the synthesis of AuNP. Moreover, it was observed that the SPR and fluorescence emission of AuNP can be tuned by varying reactant concentration and temperature. The present method reported the production of AuNP at a temperature below 100^0C and hence it could be regarded as semi-green method compared to the conventional method, which requires sodium borohydrate or sodium citrate as reducing agent. Furthermore, our process could save huge energy consumption, which can be used in the industry for a possible technique towards mass production of AuNP at a relatively cheaper cost.

Furthermore, we demonstrated the colorimetric as well as SPR detection based sensing for heavy metal by AuNP. We proved that starch capped AuNP could demonstrate SPR and colorimetric based sensing ability for Cu^{2+} and Pb^{2+} within 10 min. Although, colorimetric sensing of $Ni^{2+,}$ Zn^{2+}, As^{5+}, and Hg^{2+} was not significant, SPR shift was significant. Hence, we concluded that precise use of both starch and NaOH could synthesize AuNP with desired size and tunable optical properties and such NP can be used as colorimetric sensor for specific heavy metal sensing (Here Cu^{2+} and Pb^{2+}) in contaminated water. Moreover, our AuNP can also be used for the applications like medical imaging, developing biosensors and drug delivery system.

Acknowledgement

The authors thank the Department of Biotechnology, Government of India for financial support, and National Institute of Technology, Government of India, for infrastructural support. The Authors also thank Indian Institute of Technology Bombay for providing Electron Microscopy facility.

References:

1. E. Hutter and D. Maysinger, *Trends Pharmacol. Sci.*, 2013, **34**, 497-507.
2. T. Špringer, M. L. Ermini, B. Špačková, J. Jabloňků and J. Homola, *Anal. Chem.*, 2014, **86**, 10350-10356.
3. P. Cui, S. Seo, J. Lee, L. Wang, E. Lee, M. Min and H. Lee, *ACS Nano*, 2011, **5**, 6826-6833.

4. H. M. Osorio, P. Cea, L. M. Ballesteros, I. Gascon, S. Marques-Gonzalez, R. J. Nichols, F. Perez-Murano, P. J. Low and S. Martin, *J. Mater. Chem.C*, 2014, **2**, 7348-7355.
5. E. Boisselier and D. Astruc, *Chem. Soc. Rev.*, 2009, **38**, 1759-1782.
6. S. M. Moghimi, A. C. Hunter and J. C. Murray, *FASEB J.*, 2005, **19**, 311-330.
7. Y. Q. Du, X. X. Yang, W. L. Li, J. Wang and C. Z. Huang, *RSC Adv.*, 2014, **4**, 34830-34835.
8. J. Cheng, Y. J. Gu, S. H. Cheng and W. T. Wong, *J. Biomed. Nanotech.*, 2013, **9**, 1362-1369.
9. D. Pissuwan and T. Niidome, *Nanoscale*, 2015, **7**, 59-65.
10. S. A. Khan and A. Ahmad, *RSC Adv.*, 2014, **4**, 7729-7734.
11. A. K. Nowinski, A. D. White, A. J. Keefe and S. Jiang, *Langmuir*, 2014, **30**, 1864-1870.
12. T. Serizawa, Y. Hirai and M. Aizawa, *Langmuir*, 2009, **25**, 12229-12234.
13. K. K. Katti, V. Kattumuri, S. Bhaskaran, K. V. Katti and R. Kannan, *Int J Green Nanotech. Biomed.*, 2009, **1**, B53-B59.
14. R. k. Genç, G. Clergeaud, M. Ortiz and C. K. O'Sullivan, *Langmuir*, 2011, **27**, 10894-10900.
15. A. Fernández-Lodeiro, J. Fernández-Lodeiro, C. Núñez, R. Bastida, J. L. Capelo and C. Lodeiro, *Chem. Open*, 2013, **2**, 200-207.
16. C. Engelbrekt, K. H. Sorensen, T. Lubcke, J. Zhang, Q. Li, C. Pan, N. J. Bjerrum and J. Ulstrup, *Eur.. J. Chemphyschem.*, 2010, **11**, 2844-2853.
17. C. Engelbrekt, K. H. Sørensen, J. Zhang, A. C. Welinder, P. S. Jensen and J. Ulstrup, *J. Mater. Chem.*, 2009, **19**, 7839-7839.
18. P. Raveendran, J. Fu and S. L. Wallen, *J. Am. Chem. Soc.*, 2003, **125**, 13940-13941.
19. P. Raveendran and S. L. Wallen, 2006, 34-38.
20. N. Vigneshwaran, R. P. Nachane, R. H. Balasubramanya and P. V. Varadarajan, *Carbohydr. Res.*, 2006, **341**, 2012-2018.
21. M. H. El-Rafie, H. B. Ahmed, and M. K. Zahran, *Int. Scholar. Res. Notice*, 2014, 12.
22. P. Pienpinijtham, C. Thammacharoen, and S. Ekgasit, *Macromol. Res.*, 2012, **20**, 1281-1288.

23. X. Ji, X. Song, J. Li, Y. Bai, W. Yang and X. Peng, *J. Am. Chem. Soc.*, 2007, 129, 13939-13948.

24. H. Zhang, J.-J. Xu and H.-Y. Chen, *J. Phy. Chem. C*, 2008, 112, 13886-13892.

25. J. J. G. van Soest, D. De Wit, H. Tournois and J. F. G. Vliegenthart, *Starch - Stärke*, 1994, **46**, 453-457.

26. D. Pavia, G. Lampman and G. Kriz, *Intro. Spectro.*, Harcourt College Publishers, 2001.

27. Y. Guo, Z. Wang, W. Qu, H. Shao and X. Jiang, *Biosens. Bioelectron.*, 2011, **26**, 4064-4069.

28. Y. Kim, R. C. Johnson and J. T. Hupp, *Nano Lett.*, 2001, **1**, 165-167.

29. Y.-W. Lin, C.-C. Huang and H.-T. Chang, *Analyst*, 2011, **136**, 863-871.

30. Y. J. Li, B. Xiang and Y. M. Ni, *J. Appl. Polym. Sci.*, 2004, **92**, 3881-3885.

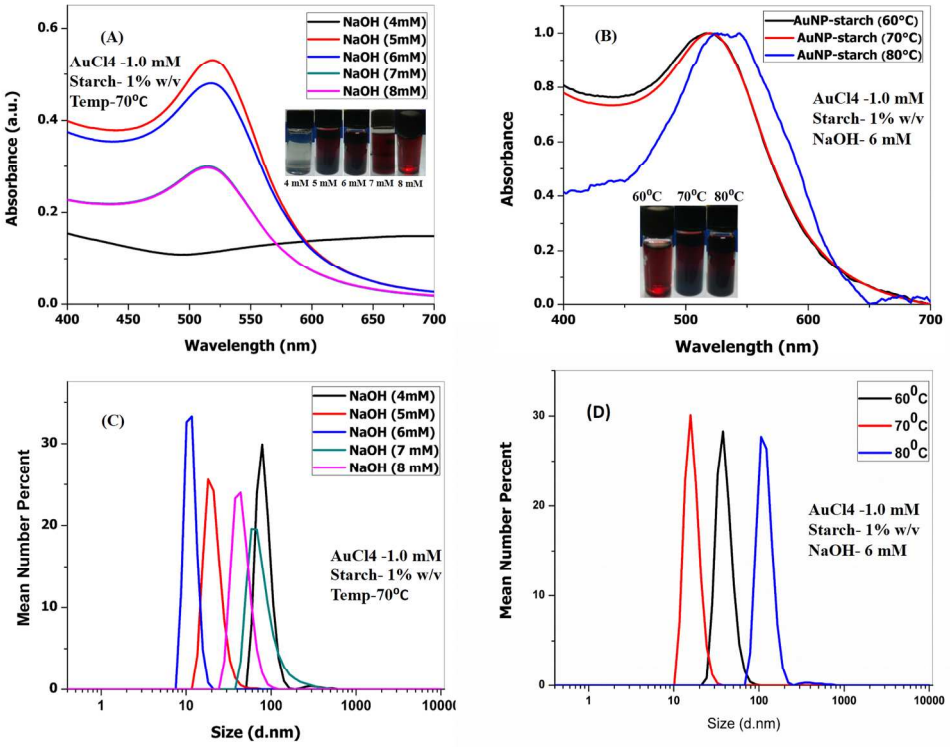

Figure 1. (A) The effect of NaOH concentration (4, 5, 6, 7, and 8 mM) on AuNP synthesis. Here, 1.0 mM auric chloride, 1% starch, and the 70^{0}C reaction temperature was used. (B) The effect of reaction temperature on the surface plasmon resonance (SPR). (C) DLS analysis of the hydrodynamic size of AuNP with various concentration of NaOH. (D) The effect of reaction temperature (60, 70, and 80 ^{0}C) in AuNP hydrodynamic size was analyzed by DLS particle size analysis.
204x163mm (300 x 300 DPI)

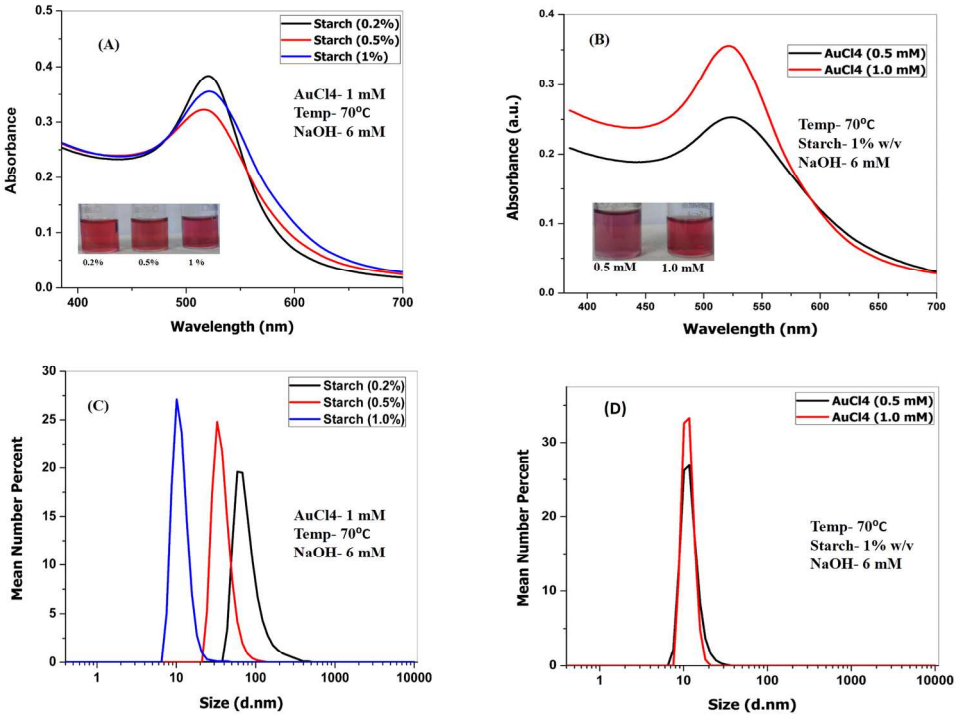

Figure 2. The effect of different concentration of starch (0.2-1%) and AuCl4 analysed. (A) SPR analysis of AuNP with different starch concentration. (B) The effect of various concentration of auric chloride (0.5-1 mM) on the the SPR. (C) hydrodynamic size of AuNP with increasing starch concentration was monitored by DLS analysis (D) DLS analysis of AuNP synthesized from 0.5 and 1.0 mM of auric chloride.
193x147mm (300 x 300 DPI)

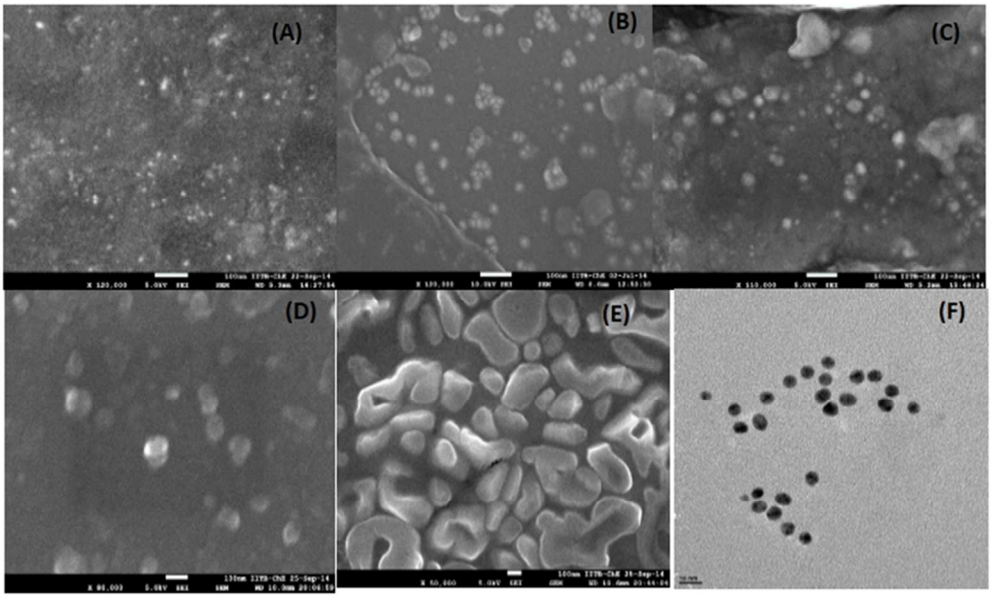

Figure 3. (A) & (B) AuNP synthesized from auric chloride (0.5 mM and 1.0 mM), 1% starch and 6 mM NaOH at 70^0C (C) auric chloride (1.0 mM), 1% starch and NaOH (8 mM) at 70^0C (D) the sample with auric chloride (1.0 mM), 1% starch and NaOH (6 mM) at 80°C; (E) AuNP-starch precipitate was observed under FESEM(Jeol) for analyze the morphology of samples. (F) The purified AuNP (1.0 mM auric chloride, 1% starch and 6 mM NaOH) at 70^0C sample prepared on a copper grid and observed under transmission electron microscope.
82x49mm (300 x 300 DPI)

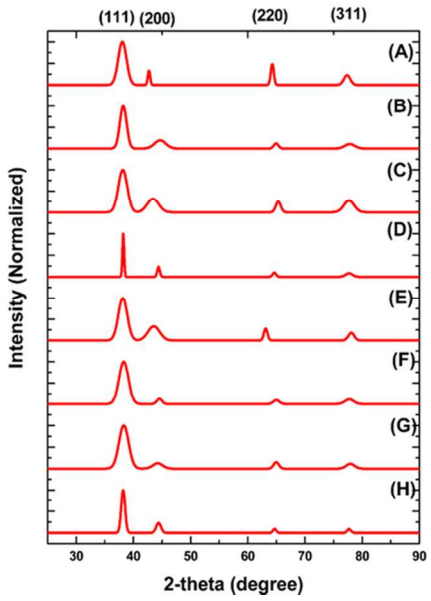

	$AuCl_4$ (mM)	NaOH (mM)	Starch (% w/v)	Temperature (°C)	Crystallite size (nm)
AuNP	1	8	1	70	14.56
AuNP	0.5	6	1	70	7.16
AuNP	1	6	1	70	7.95
AuNP	1	6	1	80	18.62
AuNP	1	6	1	60	8.68
AuNP	1	6	0.5	70	6.84
AuNP	1	6	2	70	7.55
AuNP	1	5	1	70	13.76

Figure 4. X-Ray diffraction spectra of various AuNP samples. The effect of various parameters on the characteristic peak intensity and broadening was analyzed.
82x49mm (300 x 300 DPI)

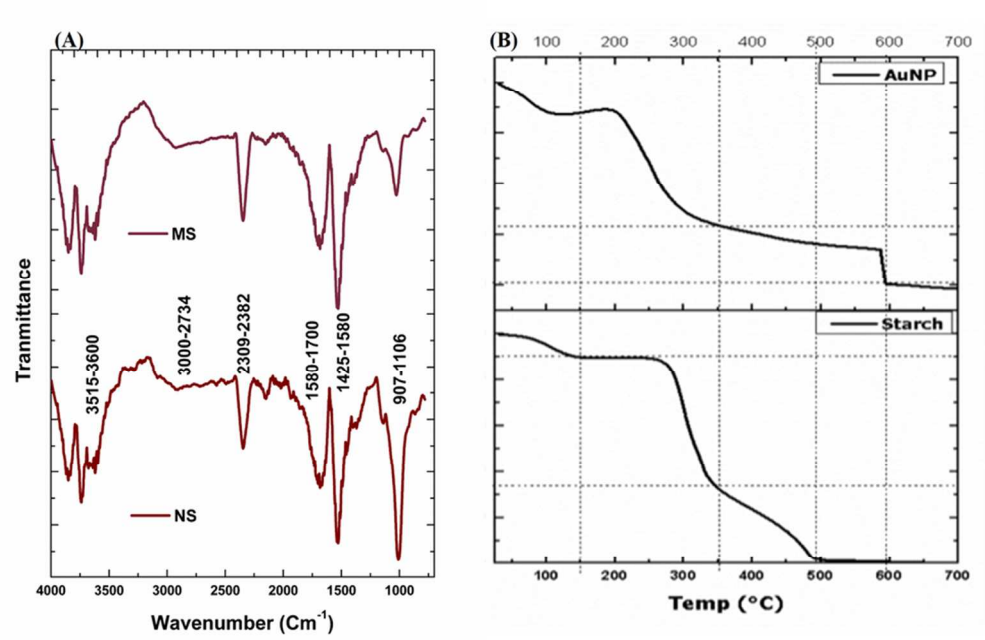

Figure 5. (A) FTIR analysis of native starch and starch after treatment with heat and 7 mM NaOH. (B) The thermal degradation analysis of starch capped AuNPs, performed in the range of 25-700^{0}C at a rate of 10°C/min.
82x54mm (300 x 300 DPI)

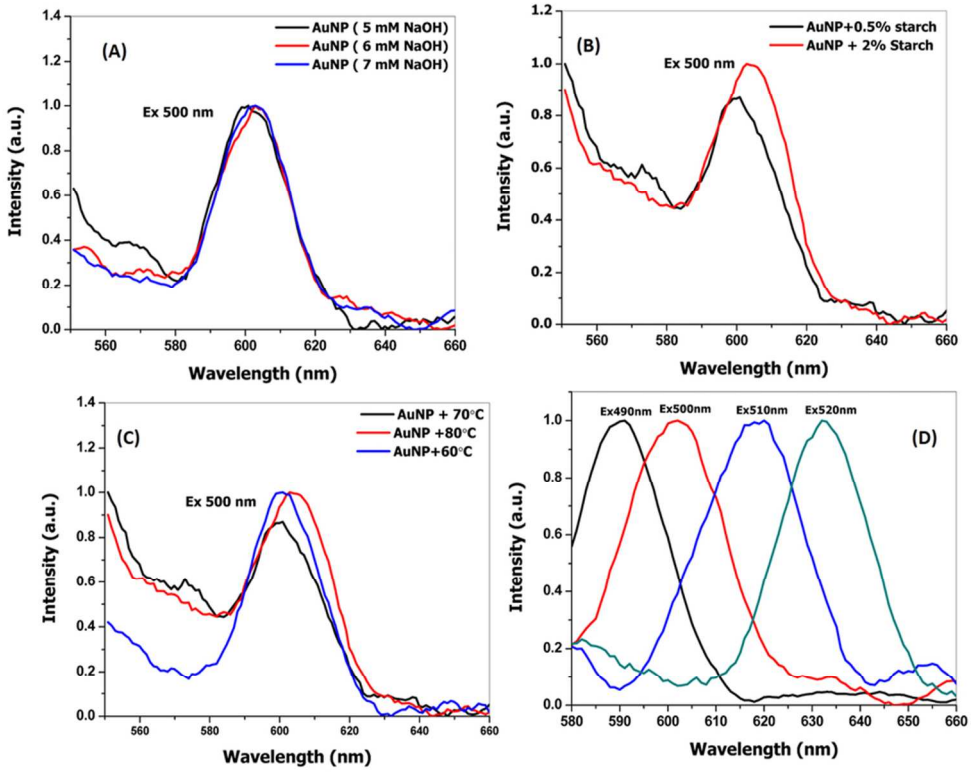

Figure 6. Fluorescence spectroscopy of AuNP samples. (A) Excitation of AuNP at 500 nm with different concentrations of NaOH (5, 6, and 7 mM). (B) AuNP sample prepared using 0.5 and 2% starch when excited at 500 nm. (C)AuNP samples synthesized at 60, 70, and 80^{0}C. (D) The AuNP samples (1.0 mM HAuCl4.3H2O, 6 mM NaOH,1% starch, 70 ^{0}C) was excited at 490, 500, 510, 520 nm. The excitation and emission slit of 10 nm each was used. The emission intensity was normalized and plotted against wavelength.
82x64mm (300 x 300 DPI)

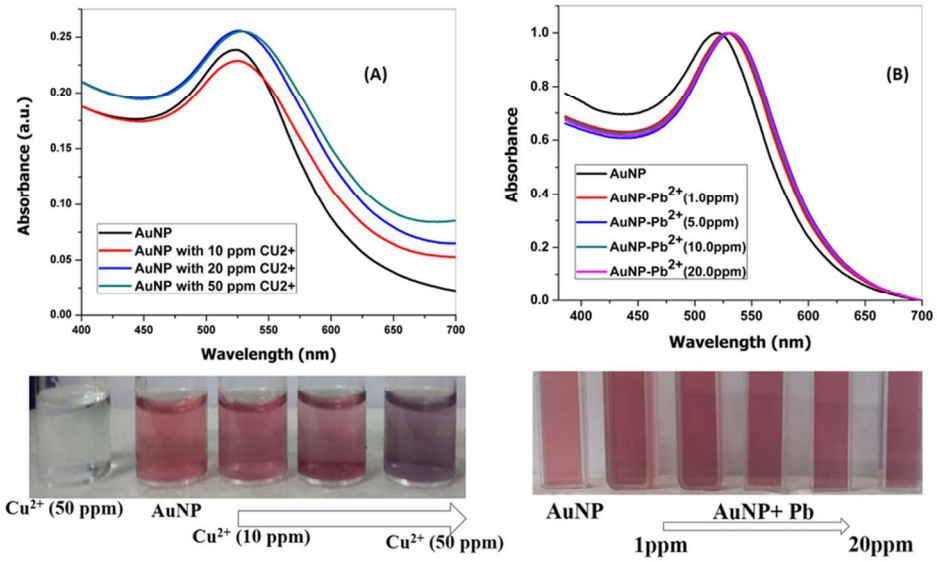

Figure 7. The effect of AuNP with different concentration of heavy metal in ppm level was analyzed. (A)The effect of AuNP (100 μM) with 10- 50 ppm of Cu2+. (B) The effect of different concentration of Pb2+ (1-20 ppm) with 70 μM of AuNP.
82x48mm (300 x 300 DPI)

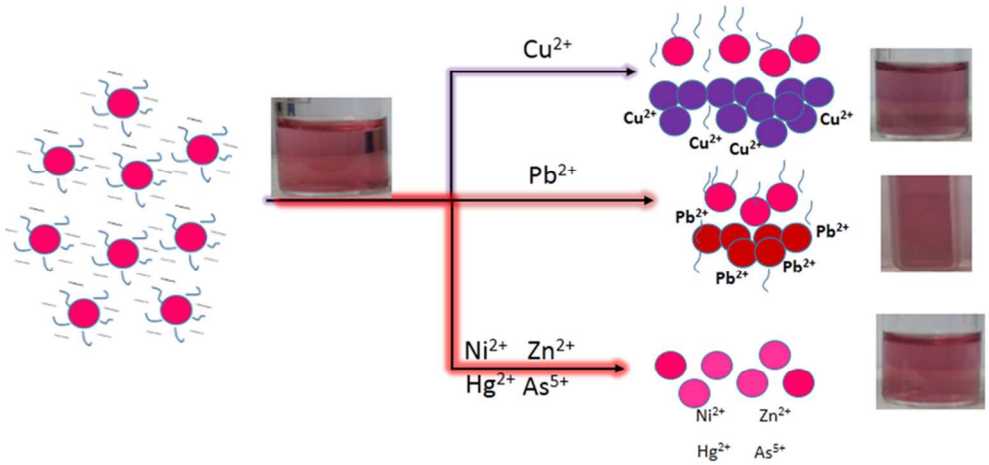

Figure 8. Schematic representation of heavy metal sensing by affinity based sensing of Cu2+, and Pb2+ byAuNP that causes aggregation of capped AuNP and color change while other four-test metal showed insignificant color change.
82x41mm (300 x 300 DPI)